

# Mott Transitions in the Hubbard Model with Spatially Modulated Interactions

Akihisa KOGA<sup>1\*</sup>, Takamitsu SAITOU<sup>1</sup>, and Atsushi YAMAMOTO<sup>2</sup>

<sup>1</sup>*Department of Physics, Tokyo Institute of Technology, Meguro, Tokyo 152-8551, Japan*

<sup>2</sup>*RIKEN, Advanced Institute for Computational Science, 7-1-26 Minatojima-minami-machi, Chuo-ku, Kobe, Hyogo 650-0047, Japan*

We study two-component fermions in optical lattices with spatially alternating on-site interactions using dynamical mean-field theory. Calculating the quasi-particle weight, double occupancy, and order parameters for each sublattice, we discuss the low-temperature properties of the system. When both interactions are repulsive, the magnetically ordered state is realized at half-filling. In the attractive case, the superfluid state is, in general, realized with a particle number imbalance. On the other hand, when repulsive and attractive interactions are comparable in the half-filled system, the magnetically ordered and superfluid states are not realized, but the metal-insulator transition occurs. This transition is characterized by the Mott and pairing transitions discussed in the conventional repulsive and attractive Hubbard models. In the doped system, commensurability emerges owing to the repulsive interactions and the metal-insulator transition occurs down to quarter-filling.

**KEYWORDS:** metal-insulator transitions, spatially modulated interactions

## 1. Introduction

Recent extensive experimental and theoretical investigations on ultracold gases have been providing a variety of interesting topics. Typical examples are ultracold atoms loaded on optical lattices with tunable and controllable parameters,<sup>1</sup> where many unusual phenomena have been observed such as the Mott transitions<sup>2-4</sup> and the crossover from the BCS-type superfluid to the Bose-Einstein condensation of tightly bound molecules.<sup>5-7</sup> Recently, the spatial modulation of the atom-atom contact interaction has been realized in the bosonic <sup>174</sup>Yb gas system,<sup>8</sup> and has been stimulating further theoretical investigations on particle correlations in ultracold atomic systems.

One of the interesting questions is how the spatial modulation in the interactions affects the low-temperature properties of fermionic optical lattice systems. Here, we consider an optical lattice with alternating on-site interactions as the simplest model. It should capture the essence of the systems with modulated interactions with a finite period. In our previous study,<sup>9</sup> we clarified that, in the half-filled system, single Mott transitions occur when the magnitudes of two interactions increase. However, it is naively expected that the magnetically ordered state or superfluid state is stabilized in the system only with repulsive or attractive interactions. Therefore, it is necessary to discuss whether or not the Mott transition is indeed realized against magnetic and superfluid fluctuations. It is also interesting to clarify how alternating interactions affect the low-temperature properties of a doped system. This should be important in discussing the low-temperature properties of realistic optical lattice systems where the local particle density varies owing to the existence of the harmonic potential.<sup>3,4,10,11</sup> On the other hand, when interacting and noninteracting sites alternate, the system is

reduced to the two-band model,<sup>12-15</sup> which has been extensively discussed in condensed matter physics. Thus, our model can be regarded as an extended version of the two-band model. Therefore, it is instructive to systematically study how low-temperature properties are affected by the spatial modulation of on-site interactions.

In this work, we consider the Hubbard model with alternating on-site interactions to discuss how particle correlations affect low-temperature properties. To this end, we make use of dynamical mean-field theory (DMFT)<sup>16-20</sup> with a continuous-time quantum Monte Carlo (CTQMC) method.<sup>21</sup> This combined method is advantageous in dealing with the magnetically ordered and superfluid states on an equal footing in the strong-coupling region. Thus, we will show how such states are affected by alternating interactions. Furthermore, we discuss the stability of the metal-insulator transition in the system.

Our paper is organized as follows. In §2, we introduce the model Hamiltonian and briefly summarize our theoretical approach. In §3, we demonstrate how the magnetically ordered and superfluid states are realized at half-filling. We clarify that the metal-insulator transition occurs in the system with both repulsive and attractive interactions. We also discuss, in §4, the effect of hole doping to clarify the role of repulsive interactions. We give a brief summary in the last section.

## 2. Model and Method

We consider two-component fermions in an optical lattice with alternating on-site interactions, which should be described by the following Hubbard Hamiltonian on a bipartite lattice:

$$H = -t \sum_{\langle ij \rangle \sigma} c_{i\sigma}^\dagger c_{j\sigma} - \sum_{i\sigma} (\mu + h\sigma) n_{i\sigma}$$

\*E-mail address: koga@phys.titech.ac.jp

$$\begin{aligned}
& + \sum_{i \in A} U_A \left( n_{i\uparrow} - \frac{1}{2} \right) \left( n_{i\downarrow} - \frac{1}{2} \right) \\
& + \sum_{j \in B} U_B \left( n_{j\uparrow} - \frac{1}{2} \right) \left( n_{j\downarrow} - \frac{1}{2} \right), \quad (1)
\end{aligned}$$

where  $c_{i\sigma}^\dagger (c_{i\sigma})$  creates (annihilates) a fermion at the  $i$ th site with spin  $\sigma$  and  $n_{i\sigma} = c_{i\sigma}^\dagger c_{i\sigma}$ .  $t$  is the hopping integral and  $U_\alpha$  is the on-site interaction at sublattice  $\alpha$  ( $= A, B$ ).  $\mu$  is the chemical potential and  $h$  is the magnetic field. Here, we note that both site-dependent interactions and potentials have been introduced in the last two terms, which can be controlled experimentally.<sup>8,22</sup>

In our model, there exists a trivial symmetry axis ( $U_A = U_B$ ), which means that the models with  $(U_A, U_B, \mu, h)$  and  $(U_B, U_A, \mu, h)$  are equivalent to each other. When  $\mu = h = 0$  ( $\langle n \rangle = 1$ ), an additional symmetry appears, where  $n = \sum_{i\sigma} n_{i\sigma}/N$  and  $N$  is the total number of sites. By applying the particle-hole transformations<sup>23</sup>  $c_{i\uparrow} \rightarrow \tilde{c}_{i\uparrow}$  and  $c_{i\downarrow} \rightarrow (-1)^i \tilde{c}_{i\downarrow}^\dagger$  to the model Hamiltonian with  $(U_A, U_B, \mu, h)$ , we obtain the model Hamiltonian with  $(-U_A, -U_B, h, \mu)$ . Therefore, in the case with  $\mu = h = 0$ , the Hubbard models with  $(U_A, U_B)$ ,  $(U_B, U_A)$ ,  $(-U_A, -U_B)$ , and  $(-U_B, -U_A)$  are identical. In the repulsive model ( $U_A > 0$  and  $U_B > 0$ ), a naively expected magnetically ordered state with a staggered moment in the  $z$ -axis ( $xy$  plane) is equivalent to the density wave (superfluid) state in the attractive model ( $U_A < 0$  and  $U_B < 0$ ). It is known that the density wave state is not stable against hole doping. Therefore, we focus on the stabilities of the magnetically ordered and superfluid states in this study. We note that the particle number imbalance ( $n_A \neq n_B$ ), which may be regarded as the density wave state, generally appears since the system has a two-sublattice structure, where  $n_\alpha = 2 \sum_{i \in \alpha, \sigma} n_{i\sigma}/N$ . In the following, we focus on the Hubbard model, eq. (1), without the magnetic field, since it is equivalent to the chemical potential under the particle-hole transformations.

The Hubbard model with alternating interactions has been studied in one-dimensional systems, where the possibility of anomalous metallic states was discussed.<sup>24,25</sup> In this paper, we deal with the infinite-dimensional Hubbard model to discuss how alternating interactions affect low-temperature properties. To clarify this issue, we employ the DMFT method.<sup>16–20</sup> In DMFT, the lattice model is mapped to an effective impurity model, where local particle correlations are taken into account precisely. The lattice Green's function is then obtained via self-consistent conditions imposed on the impurity problem. The treatment is formally exact in infinite dimensions, and even in three dimensions, DMFT successfully explains interesting physical properties such as the Mott metal-insulator transition.

When DMFT is applied to the system with a sublattice structure, Green's function is given in the Nambu formalism as<sup>26</sup>

$$\hat{G}(\mathbf{k}, z)^{-1} = \hat{G}_0(\mathbf{k}, z)^{-1} - \hat{\Sigma}(z), \quad (2)$$

with

$$\hat{G}_0(\mathbf{k}, z) = \begin{pmatrix} z\hat{\sigma}_0 + \mu\hat{\sigma}_z & -\epsilon_{\mathbf{k}}\hat{\sigma}_z \\ -\epsilon_{\mathbf{k}}\hat{\sigma}_z & z\hat{\sigma}_0 + \mu\hat{\sigma}_z \end{pmatrix}^{-1}, \quad (3)$$

and

$$\hat{\Sigma}(z) = \begin{pmatrix} \hat{\Sigma}_A(z) & 0 \\ 0 & \hat{\Sigma}_B(z) \end{pmatrix}, \quad (4)$$

where  $\hat{\sigma}_0$  is the identity matrix,  $\hat{\sigma}_z$  is the  $z$ -component of the Pauli matrix, and  $\epsilon_{\mathbf{k}}$  is the dispersion relation for the bare band.  $\hat{\Sigma}_\alpha(z)$  is the self-energy for the  $\alpha$ th sublattice in the Nambu formalism. The local lattice Green's function is obtained as  $\hat{G}_\alpha(z) = \int dk \hat{G}_{\alpha\alpha}(k, z)$ . Here, we use a semicircular density of states,  $\rho(x) = \frac{2}{\pi D} \sqrt{1 - (x/D)^2}$ , where  $D$  is the half-bandwidth, which corresponds to an infinite-coordination Bethe lattice. The self-consistency equation is then given by

$$\hat{g}_\alpha(z) = z\hat{\sigma}_0 + \mu\hat{\sigma}_z - \left(\frac{D}{2}\right)^2 \hat{\sigma}_z \hat{G}_\alpha(z) \hat{\sigma}_z, \quad (5)$$

where  $\hat{g}_\alpha(z)$  is the noninteracting Green's function of the effective Anderson impurity model for the  $\alpha$ th sublattice.

There are various numerical methods for solving the effective impurity problem, such as the iterative perturbation theory<sup>27,28</sup> and exact diagonalization.<sup>14</sup> Here, to discuss low-temperature properties quantitatively, we use the CTQMC method.<sup>21</sup> This technique has recently been developed<sup>21</sup> and has successfully been applied to general classes of models such as the Hubbard model,<sup>29–31</sup> periodic Anderson model,<sup>32,33</sup> Kondo lattice model,<sup>34</sup> and Holstein-Hubbard model.<sup>35</sup> Here, we use the hybridization-expansion version of the CTQMC method<sup>29</sup> extended to the Nambu formalism.<sup>36</sup> This allows us to directly access the superfluid state at low temperatures. In our CTQMC simulations, we measure normal and anomalous Green's functions on a grid of 1000 points. Furthermore, we also use the numerical renormalization group (NRG) method<sup>37</sup> to discuss the stability of the normal metallic state complementary. In the NRG, one discretizes the effective bath on a logarithmic mesh by introducing the discretization parameter  $\Lambda$ . The resulting discrete system can be mapped to a semi-infinite chain with exponentially decreasing couplings, which allows us to access and discuss properties involving exponentially small energy scales.<sup>38</sup> To ensure that sum rules for dynamical quantities are fulfilled, we adopt the complete-basis-set algorithm.<sup>39–41</sup> We observe that obeying the sum rules is mandatory to properly describe the low-energy properties of the system away from half-filling. In the NRG calculations, we use the discretization parameter  $\Lambda = 2$  and maintain 4000 states at each step.

In this work, we use the half-bandwidth  $D$  as the unit of energy. To discuss low-energy properties of the system with alternating interactions systematically, we calculate the quasi-particle weight  $z_\alpha = (1 - \partial \text{Re} \Sigma_\alpha(\omega)/\partial \omega)^{-1}$ , double occupancy  $D_\alpha = \langle n_{\alpha\uparrow} n_{\alpha\downarrow} \rangle$ , magnetization  $m_\alpha = (n_{\alpha\uparrow} - n_{\alpha\downarrow})/2$ , and pair potential  $\Delta_\alpha = \langle c_{\alpha\uparrow} c_{\alpha\downarrow} \rangle$  for each sublattice. When the CTQMC method is used as an impurity solver, we calculate the quantity  $z_\alpha =$

$(1 - \text{Im}\Sigma_\alpha(i\omega_0)/\omega_0)^{-1}$  as the quasi-particle weight at finite temperatures, where  $\omega_0 = \pi/\beta$ . Furthermore, by applying the maximum entropy method<sup>42-44</sup> to Green's functions, we deduce the spectral functions, thus allowing us to discuss static and dynamical properties of the systems.

### 3. Results at Half-Filling

We first discuss the low-temperature properties of the Hubbard model at half-filling.<sup>9</sup> Note that, when  $\mu = 0$ , the local particle density at each sublattice is always unity ( $n = n_A = n_B = 1$ ) since alternating interactions have been introduced together with the alternating potential in the Hamiltonian eq. (1). When the signs of two interactions are the same ( $U_A U_B > 0$ ), the ordered ground state is naively expected at zero temperature. Namely, the magnetically ordered state is stabilized in the repulsive case, while the superfluid state is stabilized in the attractive case. Here, we consider the Hubbard model with repulsive interactions, since the attractive model at half-filling is equivalent under the particle-hole transformation, as discussed above. To clarify how the magnetically ordered state is affected by alternating on-site interactions at low temperatures, we calculate the staggered magnetization  $m_{AF} = \sum_i (-1)^i m_i / N$ . The results obtained at  $T/D = 0.05$  are shown in Fig. 1. In the

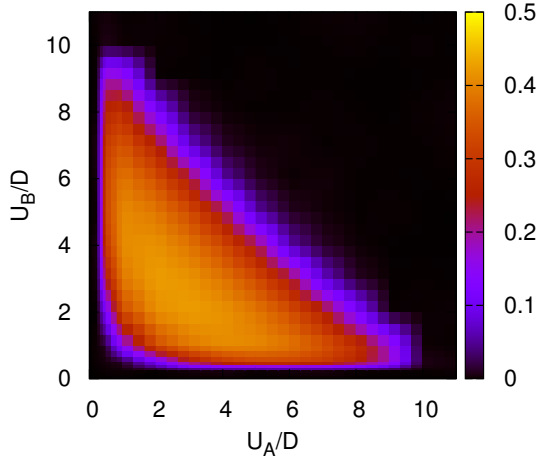


**Fig. 1.** (Color online) Density plot of the spontaneous magnetization in the system with  $T/D = 0.05$ .

weak-coupling region, the paramagnetic metallic state is realized with  $m_{AF} = 0$ . Increasing the interactions at both sublattices, the staggered magnetization is induced and the phase transition occurs to the magnetically ordered state. In this state, the magnitude of magnetization is almost uniform in the system even with alternating interactions ( $U_A \neq U_B$ ), although the Green's functions strongly depend on the sublattices. A further increase in the interactions leads to another phase transition to the paramagnetic state since thermal fluctuations are relatively enhanced in comparison with magnetic fluctuations. Since the effective intersite coupling should be scaled as  $t^2/(U_A + U_B)$ , the phase boundary is almost lin-

ear ( $U_A + U_B = \text{const.}$ ) at finite temperatures, as shown in Fig. 1.

When the temperature is lowered, the magnetically ordered state becomes more stable in the weak- and strong-coupling regions. Here, we discuss the stability of the magnetically ordered state when one of the interaction strengths is changed in the weak-coupling region. In Fig. 2, we show the spontaneous magnetization in the system with a fixed  $U_B/D$  of 6.0 at  $T/D = 0.01, 0.02$ , and 0.05. When  $U_A/D > 0.5$ , the repulsive interactions

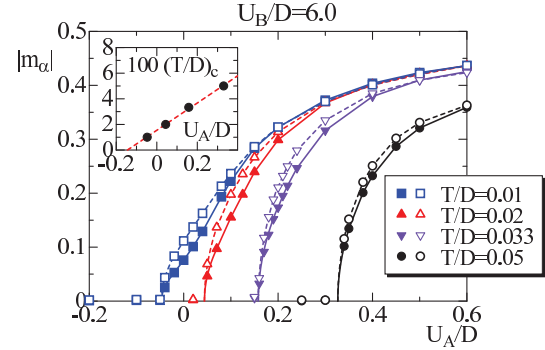


**Fig. 2.** (Color online) Solid (open) symbols represent the sublattice magnetizations  $m_A$  ( $-m_B$ ) in the system with  $U_B/D = 6.0$  at temperatures  $T/D = 0.01$  (squares), 0.02 (triangles), and 0.05 (circles).

$U_A$  and  $U_B$  cooperatively stabilize the magnetically ordered state, and the sublattice magnetizations are almost the same. Decreasing the interaction  $U_A$ , the spontaneous magnetization gradually decreases. It is found that the magnetization for sublattice  $B$  is slightly larger than that close to the critical point. This implies that the magnetically ordered state is mainly stabilized by the larger repulsive interaction  $U_B$ . A further decrease in the interaction strength induces the phase transition to the paramagnetic state, where the magnetizations simultaneously vanish. By examining the critical behavior  $|m_{AF}| \sim |U_A - (U_A)_c|^\beta$  with the exponent  $\beta = 1/2$ , we obtain the critical points as  $(U_A/D)_c \sim 0.33, 0.044$ , and  $-0.047$  at  $T/D = 0.05, 0.02$ , and  $0.01$ , respectively. By applying the least-squares method to the above critical points, we determine the quantum phase transition point  $(U_A/D)_c$  to be  $\sim -0.13$ , as seen in the inset of Fig. 2. This implies that the magnetically ordered state is realized even when  $U_A U_B < 0$ , as long as the attractive interaction is much weaker than the repulsive interaction ( $|U_A| \ll |U_B|$ ) and the temperature is low ( $T/D \lesssim 0.01$ ).

On the other hand, when the absolute values of two interactions are comparable, a nonmagnetic state is realized. To discuss the low-temperature properties of the system with fixed ratio  $U_B/U_A = -2$ , we calculate the quasi-particle weights for both sublattices at  $T/D = 0.02$ , as shown in Fig. 3. When the interactions are turned on, the quasi-particle weights  $z_A$  and  $z_B$  decrease from unity in slightly different ways reflecting the difference between on-site interactions. Namely, a strong renormalization appears in sublattice  $B$ . A further increase in the

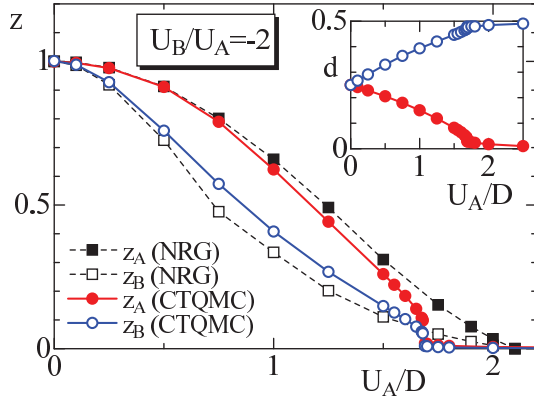


**Fig. 3.** (Color online) Quasi-particle weight for each sublattice as a function of  $U_A/D$  with fixed ratio  $U_B/U_A = -2$ . Solid lines with circles are obtained from DMFT by the CTQMC method at  $T/D = 0.02$ . Dashed lines with squares are obtained from DMFT by the NRG method. The inset shows the double occupancy in the system.

interactions induces the jump singularity in both curves at around  $U_A/D \sim 1.7$ . Then the double occupancy approaches zero (half) at sublattice  $A$  ( $B$ ), as shown in the inset of Fig. 3. These imply that the first-order phase transition to the insulating state occurs, where the singly occupied states with spin are realized at sublattice  $A$ , while the empty or doubly occupied states are equally realized at sublattice  $B$ . Therefore, we conclude that the Mott and pairing transitions simultaneously occur in sublattices  $A$  and  $B$ , respectively.

To confirm this, we show the density of states at each sublattice at  $T/D = 0.02$  in Fig. 4. It is found that two

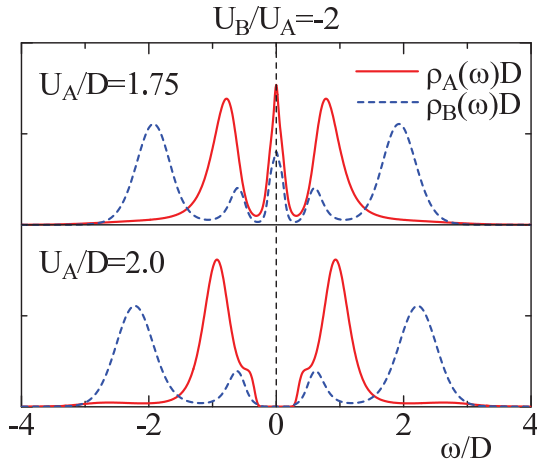


**Fig. 4.** (Color online) Solid (dashed) lines represent the density of states for sublattice  $A$  ( $B$ ). The upper (lower) panel shows the results for the metallic state with  $U_A/D = 1.75$  (the insulating state with  $U_A/D = 2.0$ ) in the system with  $U_B/U_A = -2$  at  $T/D = 0.02$ .

kinds of broad peaks appear in the high-energy region. One of them is located at around  $\omega \sim \pm U_\alpha/2$ , which forms the Hubbard gap due to the local Coulomb interactions. The other broad peak at around  $\omega \sim \pm U_{\bar{\alpha}}/2$

is induced by the on-site interaction at nearest neighbor sites, although it may be invisible on this scale for the density of states  $\rho_A$ . When  $U_A/D = 1.75$ , the sharp quasi-particle peaks for both sublattices appear near the Fermi level, which implies that the system is in the metallic state close to the Mott transition point. On the other hand, when  $U_A/D = 2.0$ , the gap structure appears in both sublattices, which means that the insulating state is induced by the Mott and pairing transitions. Therefore, we conclude that the single metal-insulator transition indeed occurs in the system with alternating interactions.

To examine the nature of the phase transition in the paramagnetic state, we also apply the NRG method as an impurity solver. In the weak-coupling region, the NRG results are in good agreement with the CTQMC results, as shown in Fig. 3. However, with increasing interactions, the quasi-particle weights do not have the jump singularity, and smoothly reach zero at the same critical point ( $U_A/D \sim 2.1$ ), which is consistent with the critical point  $U_A/D = 3/\sqrt{2}$  obtained by the linearized DMFT method.<sup>45</sup> This suggests the existence of a second-order quantum phase transition in the half-filled Hubbard model with alternating interactions, which is similar to the nature of the conventional Mott transition in the paramagnetic state.

We have discussed the low-temperature properties of the infinite-dimensional system with attractive and repulsive interactions. It has been clarified that when both interactions are comparable, superfluid and magnetic fluctuations are suppressed and the paramagnetic phase transition to the insulating state with a high residual entropy against any ordered states occurs, at least, at the temperature  $T/D = 0.02$ . Since the competition between the superfluid and magnetically ordered states can be regarded as a sort of frustration, the appearance of the residual entropy in the insulating state discussed here is similar to that in the Mott insulating state in the frustrated Hubbard model in infinite dimensions. By contrast, in the low-dimensional systems, the effective next-nearest-neighbor interactions between the same sublattices, which are beyond the DMFT framework based on our local approximation with two sublattice structures, may realize the magnetically ordered and/or superfluid (density wave) states.<sup>24</sup> In this case, its energy scale  $t^4/\bar{U}^3$  is much lower than the effective on-site interaction  $\bar{U}$ . Therefore, we can say that the metal-insulator transition discussed here is indeed realized in infinite dimensions, and even in finite dimensions it is realized at an intermediate temperature.

In the following, we discuss how alternating interactions affect low-temperature properties in the doped system.

#### 4. Hole-Doping Effects

In the section, we discuss the hole-doping effect on the system with alternating interactions. First, we consider the system only with repulsive interactions. It is known that the phase-separated magnetically ordered state is realized in the conventional Hubbard model close to half-filling at zero temperature.<sup>46</sup> To study how the spatial



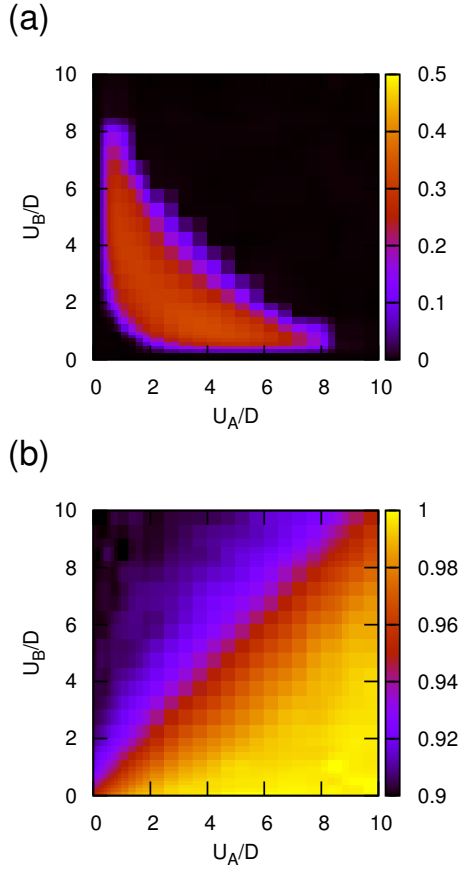


**Fig. 5.** (Color online) Density plot of spontaneous magnetization (a) and particle density in sublattice A (b) for the doped system ( $n = 0.95$ ) at  $T/D = 0.05$ .

modulation in the interactions affects the magnetic structure at low temperatures, we calculate the magnetization  $m_{AF}$  in the system with  $n = 0.95$ , as shown in Fig. 5(a). The magnetization is monotonically decreased by hole doping, in comparison with the half-filled case (see Fig. 1). It is also found that the phase boundary in the strong-coupling region is somewhat curved. This behavior should be related to the particle occupation in each sublattice. Figure 5(b) shows the particle density for sublattice A. It is found that commensurability emerges in sublattice A ( $n_A \sim 1$ ) when  $U_A \gg U_B$ . In this region, magnetic correlations are enhanced easily, which results in the curved phase boundary. In this case, the DMFT iterations converged well and we could not observe phase separation at  $T/D = 0.05$ . It is expected that the phase separation occurs at lower temperatures.<sup>46</sup> Further hole doping suppresses magnetic correlations, which leads to the phase transition to the paramagnetic state.

By contrast, it is known that, in the attractive case, the superfluid state is stable against hole doping and phase separation does not occur. To clarify how alternating interactions affect the superfluid state, we deal with the attractive Hubbard model with  $n = 0.75$  and  $U_B/U_A = 5$ . Calculating the particle density and pair potential, we obtain the results at fixed temperatures  $T/D = 0.02$  and  $0.05$ , as shown in Fig. 6. The paramagnetic metallic state is realized below a certain critical in-

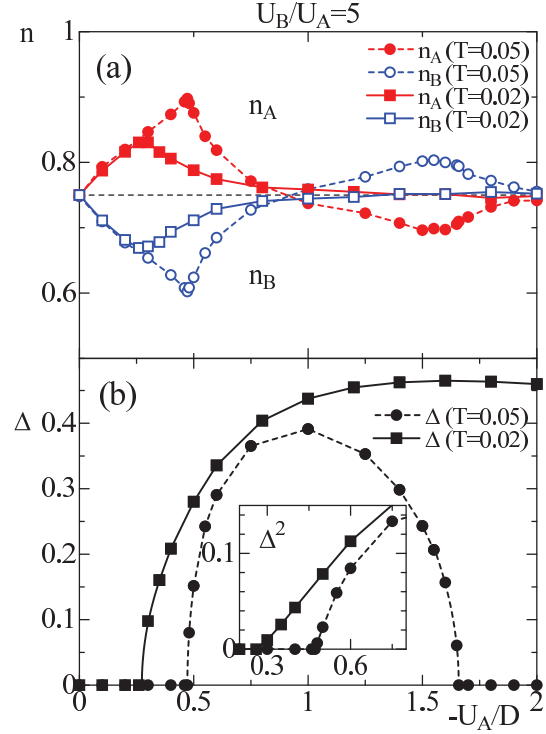


**Fig. 6.** (Color online) Particle density for each sublattice (a) and pair potential (b) as a function of  $U_A/D$  with fixed ratio  $U_B/U_A = 5$ . Solid (open) symbols are the results for sublattice A (B) obtained on the basis of DMFT by the CTQMC method.

teraction  $(U_A)_c$ , and the particle density imbalance arises with  $n_A \neq n_B$ , as shown in Fig. 6(a). In this case, the Hubbard gap ( $\sim |U_B|$ ) appears in the density of states for sublattice B, while a low-energy peak clearly appears in sublattice A, as shown in Fig. 7. Beyond the critical

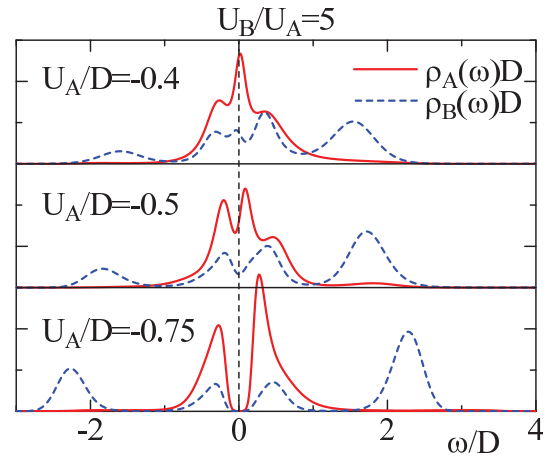


**Fig. 7.** (Color online) Density of states obtained on the basis of DMFT by the CTQMC method for  $U_A/D = -0.4, -0.5$ , and  $-0.75$  at  $T/D = 0.05$ .

interaction  $(U_A)_c$ , the pair potential  $\Delta$  is induced and the superfluid state is realized. Then a dip structure appears in the vicinity of the Fermi level, as shown in Fig. 7. Upon decreasing the temperature, the dip structure

should continuously change to the gap structure. By examining the critical behavior  $\Delta \sim |U_A - (U_A)_c|^\beta$ , we determine the critical interactions  $(U_A/D)_c = 0.47$  at  $T/D = 0.05$  and  $(U_A/D)_c = 0.27$  at  $T/D = 0.02$ , as shown in the inset of Fig. 6(b). It is also found that the particle number imbalance is suppressed once the system enters the superfluid state, as shown in Fig. 6(a). Furthermore, the particle number imbalance is almost zero when the superfluid order parameter is maximum. Since this tendency is clearly observed at low temperatures, we can say that the realization of the superfluid state makes the system uniform. Similar behavior can be found in the half-filled Hubbard model with a uniform attractive interaction where the hole doping destabilizes the density wave state and the genuine superfluid state is stabilized.

When  $U_A U_B < 0$ , interesting behavior is exhibited in the doped system ( $n = 0.75$ ). The results for the system

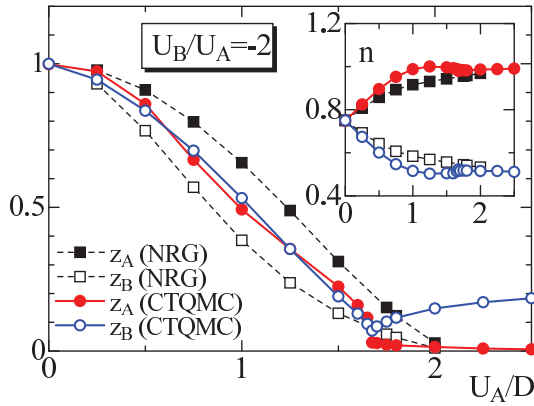


**Fig. 8.** (Color online) Quasi-particle weight for each sublattice as a function of  $U_A/D$  with fixed ratio  $U_B/U_A = -2$ . Solid lines with circles represent results obtained on the basis of DMFT by the CTQMC method at  $T/D = 0.02$ . Dashed lines with squares represent results obtained on the basis of DMFT by the NRG method. The inset shows the particle density for each sublattice.

with the fixed ratio  $U_B/U_A = -2$  at  $T/D = 0.02$  are shown in Fig. 8. The increase in the interactions monotonically decreases the quasi-particle weight for each sublattice and a singularity appears at  $U_A/D \sim 1.7$ , which is similar to the half-filled case. However, a further increase in the interaction leads to different behavior. In sublattice A, the quasi-particle weight becomes almost zero and the local particle density becomes close to half-filling, as shown in the inset of Fig. 8. Our results suggest the existence of the Mott transition in sublattice A. In fact, the Mott gap clearly appears in the density of states, as shown in Fig. 9. By contrast, in sublattice B, the local particle density becomes far from half-filling. Then the quasi-particle weight increases beyond the transition point and the gap structure appears around the Fermi level. This behavior is characteristic of the spin-gap state induced by the pairing transition in the doped system.<sup>47</sup> Therefore, we can say that even in the doped system, the Mott and pairing transitions occur at finite temperatures.

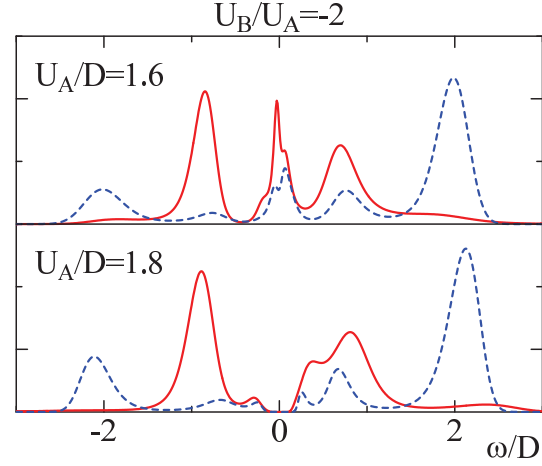


**Fig. 9.** (Color online) Density of states for the system with  $U_B/U_A = -2$  at  $T/D = 0.02$  obtained on the basis of DMFT by the CTQMC method when  $U_A/D = 1.6$  (upper panel) and 1.8 (lower panel).

However, the nature of the phase transition at zero temperature may not be trivial since, in the system with uniform interactions, the Mott transition is of the second order at half-filling and the pairing transition is of the first order far from half-filling. To clarify the stability of the normal metallic state, we calculate the renormalization factors at zero temperature by the NRG method. We see in Fig. 8 that the quasi-particle weights smoothly decrease up to  $U_A/D \sim 2.0$ . In this case, a large difference appears between the NRG and CTQMC results, in contrast to the half-filled case. This originates from the fact that the particle number at each sublattice is sensitive to the interaction strength and thermal fluctuations. When the interaction is strong enough, oscillation behavior is exhibited in the DMFT iterations and we do not find a stable solution. This implies that the first-order phase transition occurs and the phase separation is realized at zero temperature, which has been discussed for the attractive Hubbard model.<sup>47</sup> This point thus remains an open issue for future studies.

To clarify the roles of the attractive and repulsive interactions in the doped system, we also consider the system with  $U_B/U_A = -1/2$ , where the magnitude of the attractive interactions is lower than that of the repulsive interactions. Figure 10 shows that when  $U_A/D \sim 1$ , the renormalization factor in sublattice A is rapidly decreased, while that in sublattice B is hardly decreased. This behavior is in contrast to that in the case of  $U_B/U_A = -2$  (see Fig. 8), and means the absence of the symmetry axis ( $U_A = -U_B$ ). On the other hand, when the system approaches the phase transition point, the particle number for sublattice A with repulsive interactions approaches half-filling and both quasi-particle weights decrease. Finally, the singularity appears in the curves of the quasi-particle weights at  $U_A/D \sim 3.3$ , where the Mott and pairing transitions occur simultaneously. Therefore, the nature of the phase transition in the doped system is essentially the same as that in the half-filled case. Note that this is in contrast to the low-temperature behavior

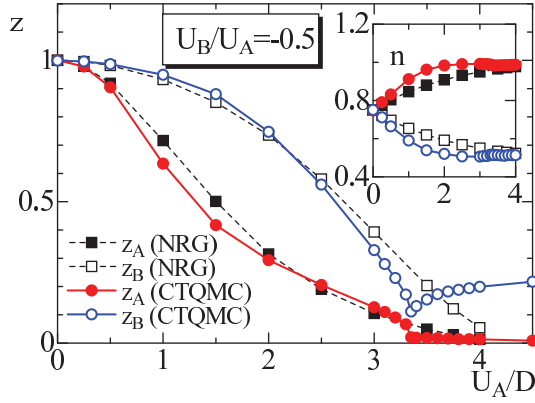


**Fig. 10.** (Color online) Quasi-particle weight for each sublattice as a function of  $U_A/D$  with fixed ratio  $U_B/U_A = -1/2$ . Solid lines with circles represent results obtained on the basis of DMFT by the CTQMC method at  $T/D = 0.02$ . Dashed lines with squares represent results obtained on the basis of DMFT by the NRG method. The inset shows the particle density for each sublattice.

in the doped system with both repulsive interactions. In such a system, the stronger repulsive interaction tends to recover the commensurability in the corresponding sublattice, but the weaker one never induces the phase transition in the case of intermediate band filling. Then the heavy metallic state is realized in the strong-coupling regime. Therefore, we can say that the single phase transition discussed here is stabilized by two effects: the Mott transition together with the commensurability due to the repulsive interaction and the pairing transition induced by the attractive interaction.

When the particle number is smaller than quarter-filling ( $0 < n < 0.5$ ), it is expected that the commensurability never arises and no phase transition occurs. To confirm this, we show the renormalization factors in the systems with  $n = 0.4$  and  $0.6$  at  $T/D = 0.02$  in Fig. 11. In the case of  $n = 0.6$ , a singularity appears at around

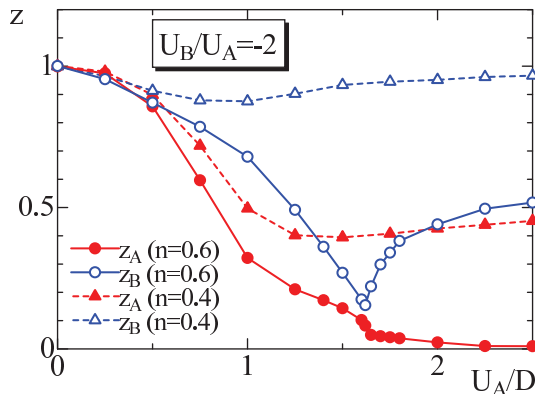


**Fig. 11.** (Color online) Quasi-particle weight for each sublattice as a function of  $U_A/D$  with fixed ratio  $U_B/U_A = -2$  at  $T/D = 0.02$ . Circles (triangles) show the results for  $n = 0.6$  ( $0.4$ ), obtained on the basis of DMFT by the CTQMC method.

$U_A/D \sim 1.6$ , which suggests the existence of the single phase transition. On the other hand, when  $n = 0.4$ , no

singularity appears in the curves of the renormalization factors. Therefore, in the doped system with  $n \leq 0.5$ , the commensurability never arises and no Mott transition occurs.

In this paper, we have discussed how spatially modulated interactions affect the low-temperature properties of an optical lattice system, being motivated by the results of recent experiments on the bosonic  $^{174}\text{Yb}$  gas system.<sup>8</sup> In the case of fermionic optical lattices, on the other hand, various parameters are highly controllable,<sup>48</sup> and the spatial modulation in the interaction should be an attractive subject of research. In this sense, our model Hamiltonian eq. (1) should capture the essence of two-component ultracold fermions in optical lattices having modulated interactions with a finite period, which will be realized in the future. By studying low-temperature properties systematically, we have clarified the role of repulsive and attractive interactions in the lattice model. Among them, in the doped system with both interactions, we found that the repulsive interaction plays a crucial role in stabilizing the metal-insulator transition. This is similar to the nature of the orbital-selective Mott transition in a doped multiband system,<sup>49,50</sup> where the commensurability in the narrow band arises owing to repulsive interactions.

Before closing this section, we comment on the validity of applying the DMFT method to realistic optical lattice systems. In DMFT, local correlations are correctly treated in the effective Anderson impurity model and intersite correlations are taken into account at the mean-field level. Therefore, we consider that our approach at least qualitatively describes the low-temperature properties of three-dimensional ultracold fermions, except for in the very low temperature region where the effective next-nearest-neighbor (NNN) interactions become relevant, as discussed at the end of §3. An interesting problem is how the metal-insulator transition discussed in this paper competes with the ordered state induced by the effective NNN interactions in finite dimensions, which is now under consideration.

## 5. Conclusions

We investigated a fermionic optical lattice system, which is described by the Hubbard model with alternating on-site interactions and potentials. By combining dynamical mean-field theory with the continuous-time Monte Carlo method, we studied low-temperature properties systematically, calculating the quasi-particle weight, double occupancy, and order parameters for each sublattice. It was clarified that the magnetically ordered state is realized in a half-filled system with only repulsive interactions, whereas the superfluid state is, in general, realized in the attractive case. We also found that when the repulsive and attractive interactions are comparable, the metal-insulator transitions occur against magnetic and superfluid fluctuations. In the doped system, we found that the commensurability arises owing to the repulsive interactions, and the insulating state remains at  $n > 1/2$ .

## Acknowledgment

This work was partly supported by the Global Center of Excellence Program “Nanoscience and Quantum Physics” of the Ministry of Education, Culture, Sports, Science and Technology (MEXT), Japan. The simulations were performed using some of the ALPS libraries.<sup>51</sup>

- 1) I. Bloch: *Nat. Phys.* **1** (2005) 23.
- 2) M. Greiner, O. Mandel, T. Esslinger, T. W. Hänsch, and I. Bloch: *Nature* **415** (2002) 39.
- 3) R. Jördens, N. Strohmaier, K. Günter, H. Moritz, and T. Esslinger: *Nature* **455** (2008) 204.
- 4) U. Schneider, L. Hackermüller, S. Will, Th. Best, I. Bloch, T. A. Costi, R. W. Helmes, D. Rasch, and A. Rosch: *Science* **322** (2008) 1520.
- 5) S. Jochim, M. Bartenstein, A. Altmeyer, G. Hendl, S. Riedl, C. Chin, J. Hecker Denschlag, and R. Grimm: *Science* **302** (2003) 2101.
- 6) M. W. Zwierlein, C. A. Stan, C. H. Schunck, S. M. F. Raupach, S. Gupta, Z. Hadzibabic, and W. Ketterle: *Phys. Rev. Lett.* **91** (2003) 250401.
- 7) T. Bourdel, L. Khaykovich, J. Cubizolles, J. Zhang, F. Chevy, M. Teichmann, L. Tarruell, S. J. J. M. F. Kokkelmans, and C. Salomon: *Phys. Rev. Lett.* **93** (2004) 050401.
- 8) R. Yamazaki, S. Taie, S. Sugawa, and Y. Takahashi: *Phys. Rev. Lett.* **105** (2010) 050405.
- 9) T. Saitou, A. Koga, and A. Yamamoto: arXiv:1204.4188.
- 10) A. Koga, T. Higashiyama, K. Inaba, S. Suga, and N. Kawakami: *J. Phys. Soc. Jpn.* **77** (2008) 073602; *Phys. Rev. A* **79** (2009) 013607.
- 11) M. Snoek, I. Titvinidze, C. Töke, K. Byczuk, and W. Hofstetter: *New J. Phys.* **10** (2008) 093008.
- 12) V. J. Emery: *Phys. Rev. Lett.* **58** (1987) 2794.
- 13) A. Georges, G. Kotliar, and W. Krauth: *Z. Phys. B* **92** (1993) 313.
- 14) M. Caffarel and W. Krauth: *Phys. Rev. Lett.* **72** (1994) 1545.
- 15) Y. Ohashi and Y. Ono: *J. Phys. Soc. Jpn.* **70** (2001) 2989.
- 16) W. Metzner and D. Vollhardt: *Phys. Rev. Lett.* **62** (1989) 324.
- 17) E. Müller-Hartmann: *Z. Phys. B: Condens. Matter* **74** (1989) 507.
- 18) Th. Pruschke, M. Jarrell, and J. K. Freericks: *Adv. Phys.* **44** (1995) 187.
- 19) A. Georges, G. Kotliar, W. Krauth, and M. J. Rozenberg: *Rev. Mod. Phys.* **68** (1996) 13.
- 20) G. Kotliar and D. Vollhardt: *Phys. Today* **57** (2004) 53.
- 21) E. Gull, A. J. Millis, A. I. Lichtenstein, A. N. Rubtsov, M. Troyer, and P. Werner: *Rev. Mod. Phys.* **83** (2011) 349.
- 22) S. Peil, J. V. Porto, B. L. Tolra, J. M. Obrecht, B. E. King, M. Subbotin, S. L. Rolston, and W. D. Phillips: *Phys. Rev. A* **67** (2003) 051603.
- 23) H. Shiba: *Prog. Theor. Phys.* **48** (1972) 2171.
- 24) P. Kakashvili and G. I. Japaridze: *J. Phys.: Condens. Matter* **16** (2004) 5815.
- 25) A. Yamamoto, S. Yamada, and M. Machida: private communication.
- 26) R. Chitra and G. Kotliar: *Phys. Rev. Lett.* **83** (1999) 2386.
- 27) A. Georges and G. Kotliar: *Phys. Rev. B* **45** (1992) 6479.
- 28) X. Y. Zhang, M. J. Rozenberg, and G. Kotliar: *Phys. Rev. Lett.* **70** (1993) 1666.
- 29) P. Werner, A. Comanac, L. de’ Medici, M. Troyer, and A. J. Millis: *Phys. Rev. Lett.* **97** (2006) 076405.
- 30) A. Koga and P. Werner: *J. Phys. Soc. Jpn.* **79** (2010) 064401.
- 31) N. Takemori and A. Koga: *J. Phys. Soc. Jpn.* **81** (2012) 063002.
- 32) A. Koga and P. Werner: *J. Phys. Soc. Jpn.* **79** (2010) 114401.
- 33) D. J. Luitz and F. F. Assaad: *Phys. Rev. B* **81** (2010) 024509.
- 34) J. Otsuki, H. Kusunose, P. Werner, and Y. Kuramoto: *J. Phys. Soc. Jpn.* **76** (2007) 114707; J. Otsuki, H. Kusunose, and Y. Kuramoto: *Phys. Rev. Lett.* **102** (2009) 017202.
- 35) F. F. Assaad and T. C. Lang: *Phys. Rev. B* **76** (2007) 035116; P. Werner and A. J. Millis: *Phys. Rev. Lett.* **99** (2007) 146404.
- 36) A. Koga and P. Werner: *Phys. Rev. A* **84** (2011) 023638.
- 37) R. Bulla, T. A. Costi, and Th. Pruschke: *Rev. Mod. Phys.* **80** (2008) 395.
- 38) A. Koga, N. Kawakami, R. Peters, and Th. Pruschke: *Phys. Rev. B* **77** (2008) 045120; *J. Phys. Soc. Jpn.* **77** (2008) 033704.
- 39) F. B. Anders and A. Schiller: *Phys. Rev. B* **74** (2006) 245113.
- 40) R. Peters, Th. Pruschke, and F. B. Anders: *Phys. Rev. B* **74** (2006) 245114.
- 41) A. Weichselbaum and J. von Delft: *Phys. Rev. Lett.* **99** (2007) 076402.
- 42) S. F. Gull, in *Maximum Entropy and Bayesian Methods in Science and Engineering*, ed. G. J. Erickson and C. R. Smith (Kluwer Academic, Dordrecht, 1988) p. 53; J. Skilling (Kluwer Academic, Dordrecht, 1989) p. 45; S. F. Gull, *ibid.* p. 53.
- 43) R. N. Silver, D. S. Sivia and J. E. Gubernatis: *Phys. Rev. B* **41** (1990) 2380; J. E. Gubernatis, M. Jarrell, R. N. Silver and D. S. Sivia: *Phys. Rev. B* **44** (1991) 6011.
- 44) W. F. Press, S. A. Teukolsky, W. T. Vetterling and B. R. Flannery, *Numerical Recipes* (Cambridge University Press, Cambridge, 1992) p. 809.
- 45) R. Bulla and M. Potthoff: *Eur. Phys. J. B* **13** (2000) 257.
- 46) R. Zitzler, Th. Pruschke, and R. Bulla: *Eur. Phys. J. B* **27** (2002) 473.
- 47) M. Capone, C. Castellani, and M. Grilli: *Phys. Rev. Lett.* **88** (2002) 126403.
- 48) L. Tarruell, D. Greif, T. Uehlinger, G. Jotzu, and T. Esslinger: *Nature* **483** (2012) 302.
- 49) A. Koga, N. Kawakami, T. M. Rice, and M. Sigrist: *Phys. Rev. Lett.* **92** (2004) 216402.
- 50) K. Inaba and A. Koga: *J. Phys. Soc. Jpn.* **76** (2007) 094712.
- 51) A. F. Albuquerque, F. Alet, P. Corboz, P. Dayal, A. Feiguin, S. Fuchs, L. Gamper, E. Gull, S. Gürtler, A. Honecker, R. Igarashi, M. Körner, A. Kozhevnikov, A. Läuchli, S. R. Manmana, M. Matsumoto, I. P. McCulloch, F. Michel, R. M. Noack, G. Pawłowski, L. Pollet, T. Pruschke, U. Schollwöck, S. Todo, S. Trebst, M. Troyer, P. Werner, and S. Wessel: *J. Magn. Magn. Mater.* **310** (2007) 1187.